Dynamic Balance of pSTAT1 and pSTAT3 in C57BL/6 Mice Infected with Lethal or Nonlethal *Plasmodium yoelii*

Xibao Shi[1, 2], Li Qin[1], Guangjie Liu[1], Siting Zhao[1], Nanzheng Peng[1] and Xiaoping Chen[1, 2, 3]

Signal transducer and activator of transcription (STAT) proteins play an important role in cytokine signaling pathways and regulation of immune responses. The balance of the phosphorylated (activated) STAT1 (pSTAT1) and STAT3 (pSTAT3) has been documented in cancer immunology. In this study, we investigated the dynamic balance of pSTAT1 and pSTAT3 in C57BL/6 mice infected with either a nonlethal (Py17XNL) or lethal (Py17XL) strain of *Plasmodium yoelii*. Both Py17XNL and Py17XL infections induced a maximum activation of STAT1 and STAT3 on the first day after parasite inoculation. Additionally, the Py17XNL infection induced a pSTAT1-dominant response in mice during the early stage of infection, with the resolution of parasitemia. In contrast, Py17XL infection induced a pSTAT3-dominant response during the early phase of infection, with the death of the animals. Our results indicated that maximum activation of STAT1 and STAT3 occurred much earlier than the peak levels of cytokines induced by *Plasmodium yoelii* infection based on previous reports and that infection with Py17XNL and Py17XL induced different dynamic patterns of pSTAT1 and pSTAT3 balance.

Key Words: malaria, *Plasmodium yoelii*, pSTAT1, pSTAT3

Introduction

Malaria, which is caused by the mosquito-transmitted protozoan parasite *Plasmodium* spp., is one of the major human infectious diseases and causes 1-3 million deaths per year (1). At this time, there is no effective vaccine available to control malaria partially due to the lack of a full understanding of the immune mechanisms involved in malaria immunity. Numerous studies have revealed the importance of the cytokine balance in immune protection against malaria. A Th1/pro-inflammatory cytokine (IFN-γ, IL-12 and TNF-α) response during the early stage of infection mediates protective immunity and the resolution of parasite infection (1-6). The initial pro-inflammatory response may switch to a predominant anti-inflammatory response that is mediated by immunoregulatory cytokines, such as TGF-β and IL-10 which down-regulate pro-inflammatory cytokine production to avoid malaria-associated pathology (7-12). The pro- and anti-inflammatory cytokine balance is critical in determining the outcome of malaria infection (12-15).

Signal transducer and activator of transcription (STAT) proteins are a group of proteins that transmit signals of many cytokines from the extracellular milieu into the nucleus (16, 17). These proteins locate in the cytoplasm in an inactive form and are phosphorylated (activated) by the ligand-activated Janus tyrosine kinases (JAKs) and translocated to the nucleus. STAT1, the first known member of STAT family, is a principal target of both type I and type II interferons (IFNs). It is critically involved in the initiation of Th1 inflammatory cascade (18-22). Activation of STAT1 promotes the activation of dentritic cells (DCs) (22, 23) and natural killer (NK) cells (24), and inhibits the development of regulatory T cells (25, 26). pSTAT3, which has antagonistic effect on pSTAT1 (27, 28), is not only a potent negative regulator of the Th1-mediated inflammatory response, but also an activator of many genes that are crucial for immune regulation (29, 30). Down-regulation of STAT3 could enhance Th1 type immune response and activate DCs, NK cells and macrophages (31-33). So the balance of pSTAT1 and pSTAT3, which has been studied in cancer immunity (31, 34), has an important role in regulation of immune responses. A higher pSTAT1/pSTAT3 ratio in tumor cell or in immune cell is associated with longer survival for

[1]Guangzhou Institute of Biomedicine and Health, Chinese Academy of Science, Guangzhou 510663, China;

[2]School of Life Sciences, University of Science and Technology of China, Hefei 230027, China;

[3]Corresponding to: Dr. Xiaoping Chen, Laboratory of Pathogen Biology, Guangzhou Institute of Biomedicine and Health, Chinese Academy of Sciences, Guangzhou Science Park, Guangdong 510663, China. Tel: +86-20-3229-0619; Fax: +86-20-3229-0706, E-mail: chen_xiaoping@gibh.ac.cn

tumor patients (26, 31, 35, 36). However, this balance has not been studied in malaria immunology.

The aims of the present study are to analyze the patterns of pSTAT1 and pSTAT3 responses in mice during infection with a nonlethal (Py17XNL) or lethal (Py17XL) strain of *Plasmodium yoelii*, and test our hypothesis that infections with Py17XNL and Py17XL might induce different dynamic patterns of pSTAT1 and pSTAT3 balance.

Materials and Methods

Mice, parasites and infection

Female 10- to 12-week-old C57BL/6 mice purchased from Vitalriver Experiment Animal Limited Company (Beijing, China) were bred in the Animal Center of Guangzhou Institute of Biomedicine and Health in accordance with the Guide to the Care and Use of Laboratory Animal Committee of the institute. *Plasmodium yeolii* lethal strain Py17XL was obtained from Malaria Research and Reference Reagent Resource Center (MR4, USA), and nonlethal strain Py17XNL was a gift from Dr. Yaming Cao (Department of Immunology, College of Basic Medical Sciences, China Medical University). The mice were injected intraperitoneally with 5×10^5 Py17XL or Py17XNL parasitized erythrocytes (pRBCs) from infected donor mice, and the control mice were injected with uninfected RBCs (uRBCs). Parasitemia levels were monitored by examination of Giemsa-stained thin blood smears prepared from tail blood.

Four mice infected with Py17XL were sacrificed on days 1, 3 and 7 post inoculation respectively; four mice infected with Py17XNL were sacrificed on days 1, 3, 7, 14, 21 and 28 post inoculation; and four uninfected control mice were sacrificed at the same time-points as those infected with Py17XNL. Celiac macrophages were obtained by celiac lavage with cold phosphate-buffered saline (PBS) and frozen at -80°C immediately for Western blot analysis. Mesenteric lymph nodes, livers and spleens were excised and either frozen in liquid nitrogen for Western blot analysis or fixed in formalin and embedded in paraffin for immunohisto-chemistry (IHC) analysis.

Western blot analysis

To analyze expressions of STAT1, pSTAT1, STAT3 and pSTAT3 in tissues, frozen samples were lysed in ice-cold lysing buffer (1% Nonidet P-40, 0.1% sodium deoxycholate, 0.1% SDS, 50 mM Tris-HCl (pH 7.4), 150 mM NaCl, 2 mM EDTA, 2 mM Na_3VO_4, 2 mM NaF and a protease inhibitor cocktail). The total protein concentration was quantified with the Bradford Protein Assay (Biocolor Bioscience & Technology Company, Shanghai). The proteins were separated on SDS-PAGE gels and transferred to polyvinylidene difluoride membranes (Millipore Company). Because the main objective of this study is to describe the dynamics of these proteins, we tried many times to optimize the sample concentrations and their incubation conditions. Appropriate methods were described below: 70 μg spleen extract was added for detecting pSTAT1/3 and 10 μg for detecting STAT1/3; 100 μg liver extract was added for detecting pSTAT1/3 and 20 μg for detecting STAT1/3; 50 μg mesenteric lymph node extract was added for detecting pSTAT1/3 and 10 μg for detecting STAT1/3; 40 μg celiac macrophage extract was added for detecting pSTAT1/3 and 10 μg for detecting STAT1/3. The membranes were blocked with 5% nonfat dried milk for 1 h. For detecting the expression of STAT1 and STAT3, the membranes were incubated for 1 h at room temperature with rabbit anti-mouse STAT1 (1:1,000) or rabbit anti-mouse STAT3 (1:1,000) or rabbit anti-mouse β actin (1:10,000) antibodies. For anti-phosphotyrosine blots, the membranes were first incubated for 30 min at room temperature and then incubated overnight at 4°C with rabbit anti-mouse pSTAT1$^{(Tyr701)}$ (1:1,000) or rabbit anti-mouse pSTAT3$^{(Tyr705)}$ (1:1,000) antibodies. Subsequently the membranes were incubated with appropriate secondary antibodies for 1 h. Then the membranes were treated with ECL detection solutions and exposed to films: the exposure time was about 10 min for detecting the expression of pSTAT1/3, and about 2 min for STAT1/3. Anti-β actin antibody was obtained from Zhongshan Goldenbridge Biotechnology Company (China). The other antibodies and ECL detection solutions were purchased from Cell Signaling Technology (USA).

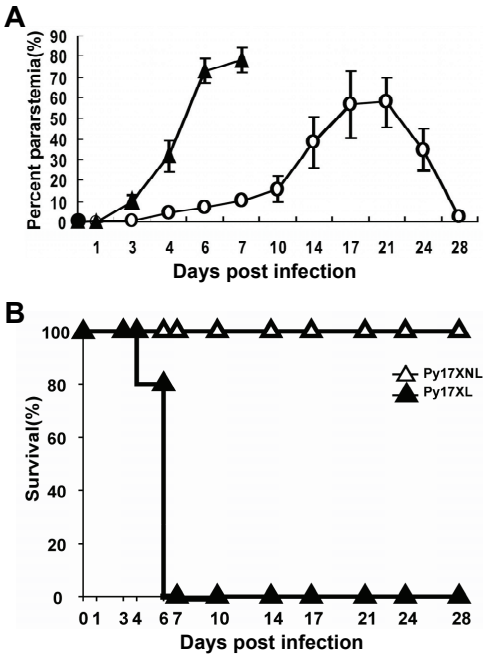

Figure 1. The course of infection with lethal (Py17XL) and nonlethal (Py17XNL) *Plasmodium yoelii* in C57BL/6 mice. (A) Parasitemia levels in C57BL/6 mice infected with 5×10^5 Py17XL (▲) or Py17XNL (○) pRBCs. The values shown are mean ± SE. (B) The survival of mice infected with Py17XL (▲) or Py17XNL (△). (n = 10)

Immunohistochemistry analysis

Spleen and liver samples were fixed in 10% buffered

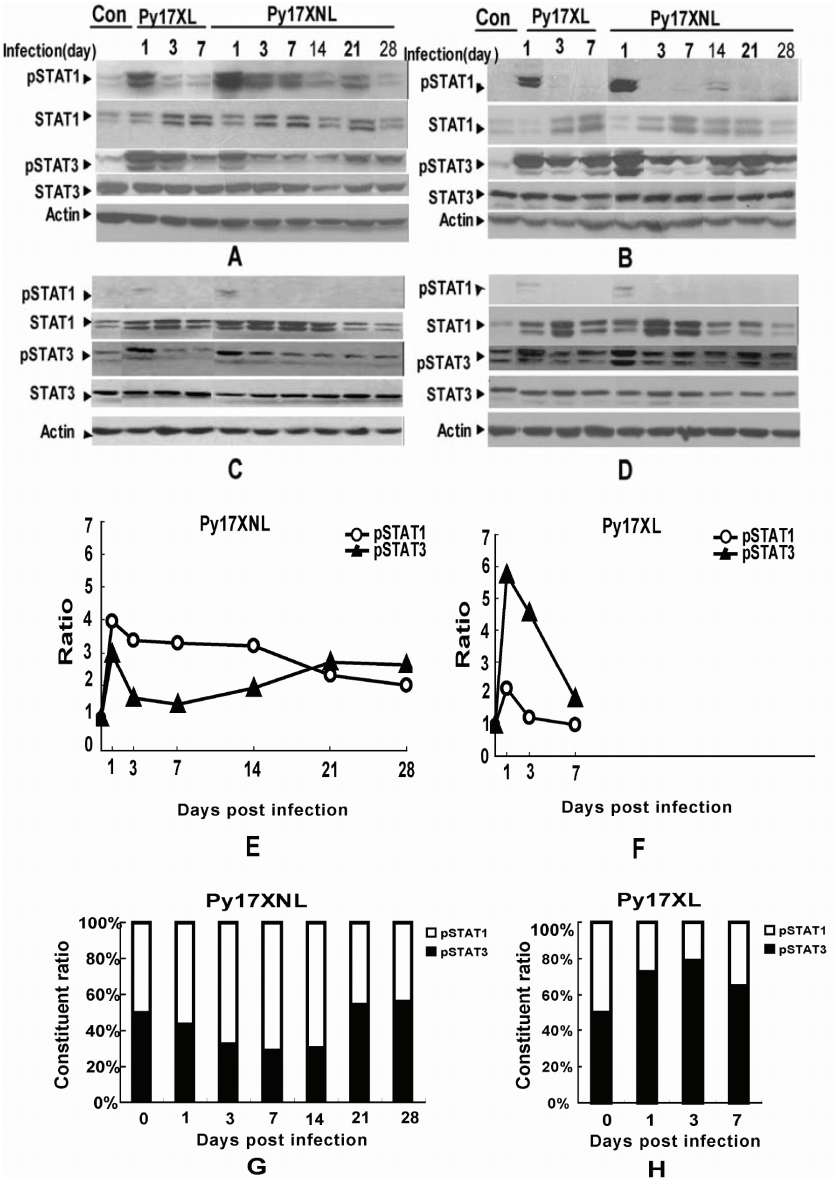

Figure 2. Expression and activation of STAT1 and STAT3 during Py17XL and Py17XNL infections. The expression levels of STAT1, STAT3, pSTAT1 and pSTAT3 in the spleen (A), liver (B), mesenteric lymph node (C) and celiac macrophages (D). Total protein was extracted from the tissues or cells, and STAT protein expression levels were analyzed by Western blot as described in Materials and Methods. The Western blot results for pSTAT1 and pSTAT3 in spleen were quantified with Quantity One Software during the whole course of malaria infection. The pSTAT1 and pSTAT3 intensities were respectively corrected by dividing by the actin intensity. The ratio of ipSTAT to conpSTAT is plotted in the figure. Ratio = (ipSTAT/Actin) / (conpSTAT/Actin). (E) The ratio of ipSTAT to conpSTAT in the spleen of mice infected with Py17XNL. (F) The ratio of ipSTAT to conpSTAT in the spleen of mice infected with Py17XL. (G) The constituent ratio of pSTAT1 and pSTAT3 in the spleen of mice infected with Py17XNL. (H) The constituent ratio of pSTAT1 and pSTAT3 in the spleen of mice infected with Py17XL. Each group at each indicated time point consisted of 4 mice, and the results were from one of three independent experiments with similar observations. Con, control; conpSTAT, pSTAT1 or pSTAT3 of the uninfected control mice; ipSTAT, pSTAT1 or pSTAT3 of the mice infected with Py17XNL or Py17XL.

formalin, embedded in paraffin, and sectioned into 3 μm sections for staining with hematoxylin and eosin (HE) or for immunohistochemical staining. The slides were de-paraffinized in xylene, rehydrated through a graded series of alcohol and washed in PBS. The sections were heated in a microwave oven for 25 min in 100 mM Tris-5% Urea (pH 9.0) and the liver sections heated in a microwave oven for 25 min in 10 mM citrate buffer (pH 6.0) to retrieve antigens. After blocking endogenous peroxidase with 0.3% hydrogen peroxide, slides were placed in 5% normal goat serum for 15 min. The primary antibodies rabbit anti-mouse pSTAT1$^{(Tyr701)}$ (1:200) and pSTAT3$^{(Tyr705)}$ (1:50) (Cell Signaling Technology) were

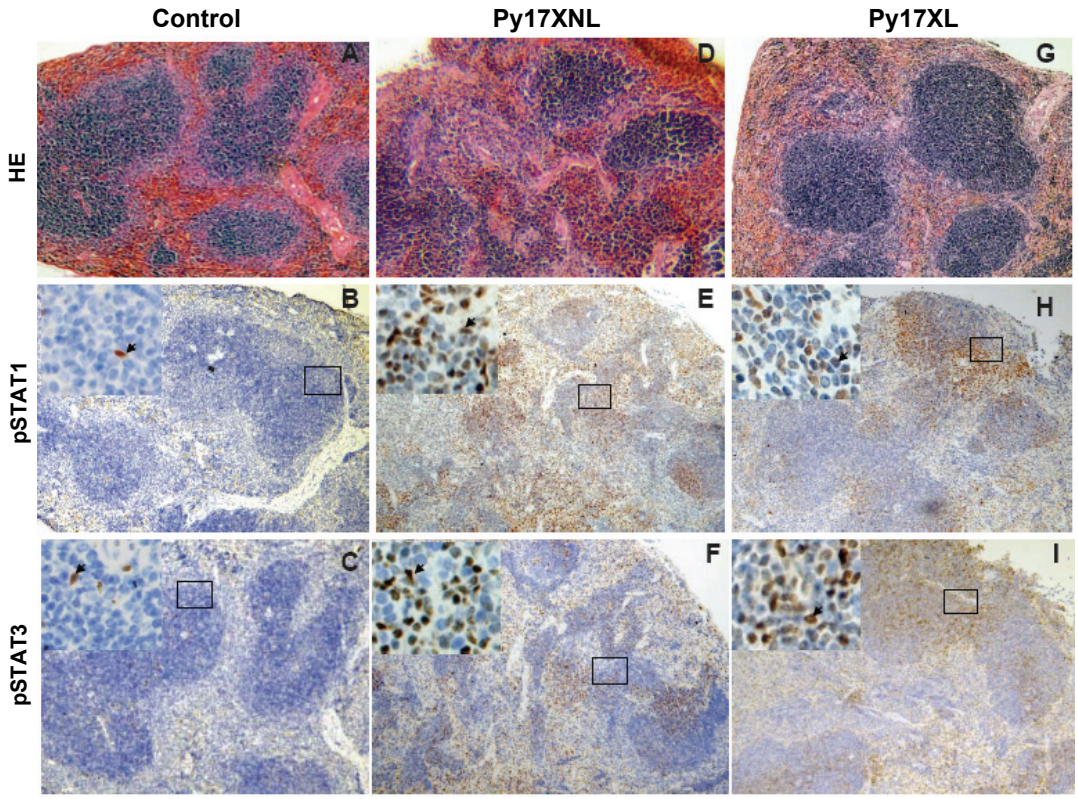

Figure 3. Immunohistochemical assay for pSTAT1 and pSTAT3 in spleens of mice on the first day after infection with Py17XL or Py17XNL. Both strains of the malaria parasite rapidly induced the activation of STAT1 and STAT3. The pSTAT1/3-positive cells (arrow) dispersed in every region, including white and red pulp. Each group at each indicated time point consisted of 4 mice, and the results were from one of three independent experiments with similar observations. Original magnifications ×50 or ×400.

applied to the slides and incubated overnight at 4°C. After incubation with biotinylated goat anti-rabbit IgG for 30 min at room temperature, each slide was incubated in the avidin-biotin peroxidase complex for 30 min at room temperature (SP-9001 kit, Zhongshan Goldenbridge Biotechnology), then each slide was reacted with substrate buffer and DAB (diaminobenzidine) chromogen. Finally, the sections were counterstained with hematoxylin (Sigma). For negative controls, an equivalent rabbit pre-immune serum was used in place of the primary antibody.

Results

Courses of infections with Py17XL and Py17XNL in C57BL/6 mice

C57BL/6 mice infected with Py17XNL developed parasitemia which increased steadily from approximately day 4 and reached a peak of parasite density (about 50% erythrocyte infected) on day 17 post inoculation (p.i.). The parasitemia then decreased, and the infection was cleared by day 28 p.i.. In contrast, infection with Py17XL resulted in a rapid increase of parasitemia that reached 80% by 7 days p.i., and all infected mice died by day 7 p.i. due to severe parasitemia (Figures 1A and 1B).

Dynamic analysis of pSTAT1 and pSTAT3 levels in mice infected with Py17XL or Py17XNL by Western blot

To analyze the activation profile of STAT1 and STAT3 during the course of Py17XL or Py17XNL infection in mice, we detected the expression levels of STAT1, STAT3, pSTAT1 and pSTAT3 in the spleen, liver, mesenteric lymph nodes and celiac macrophages.

In spleens, STAT1 expression in mice infected by both Py17XNL and Py17XL was increased, while STAT3 expression remained unchanged. Both Py17XNL and Py17XL infections induced a maximum activation of STAT1 and STAT3 (resulting in pSTAT1 and pSTAT3, the active STAT molecules) on the first day after parasite inoculation (Figure 2A). The pSTAT1 declined significantly to the baseline level on day 3 p.i. in Py17XL infected mice, whereas the level of pSTAT1 in Py17XNL infected mice declined gradually but stayed relatively higher than that of uninfected control mice till the parasites were completely eliminated. Py17XNL infection induced the level of pSTAT3 to increase on day 1 p.i., rapidly decrease on day 3 p.i., remain at a low level for 3 weeks p.i. and then to rebound to a relatively higher level afterward. In Py17XL infected mice, high pSTAT3 levels were observed until the death of the animals (Figure 2A).

Similar changes of STAT1 and STAT3 expression were

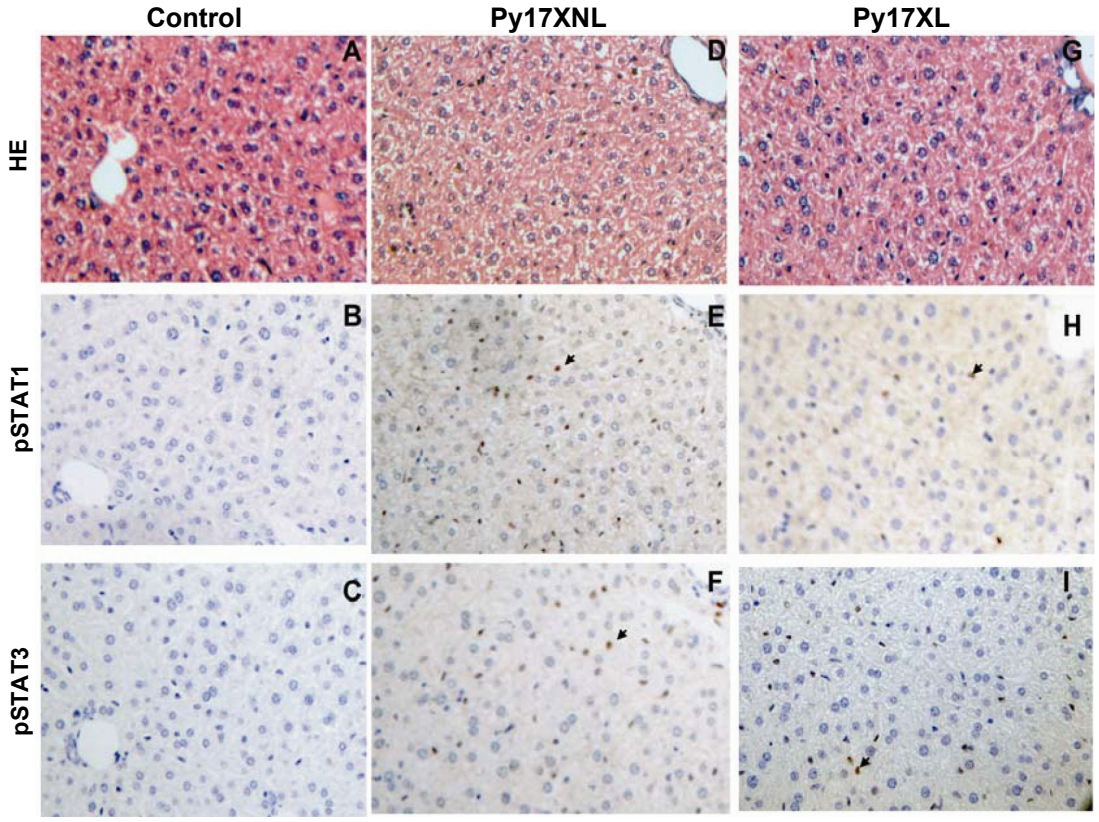

Figure 4. Immunohistochemical assay for pSTAT1 and pSTAT3 in liver tissues in mice on the first day after infection of Py17XL or Py17XNL. Both strains of the malaria parasite rapidly induced the activation of STAT1 and STAT3 (arrow). Each group at each indicated time point consisted of 4 mice, and results were from one of three independent experiments with similar observations. Original magnifications ×200.

observed in the liver (Figure 2B). In two groups of mice infected with Py17XNL and Py17XL, STAT1 expression was increased at day 3 p.i., but not at day 1 p.i.. Significant increases of pSTAT1 and pSTAT3 levels were detected on the first day p.i.. After that, pSTAT1 decreased to an undetectable level, and pSTAT3 level also declined dramatically in the following days. However, pSTAT3 in Py17XNL infected mice rebounded to a relatively higher level two weeks p.i..

Py17XNL and Py17XL infections had no effect on STAT3 expression in mesenteric lymph nodes (Figure 2C) and celiac macrophages (Figure 2D). However, STAT1 expression was increased in the short course of Py17XL infection. In Py17XNL infected mice, STAT1 expression was increased in the celiac macrophages and mesenteric lymph nodes at the first 7 and 14 days of infection respectively. In two groups of mice infected with Py17XNL and Py17XL, the changed patterns of pSTAT1 were similar to that in liver: it was detected only on the first day p.i.. Furthermore, the level of pSTAT3 in two groups increased on the first day but declined to the baseline level in the following days in both mesenteric lymph nodes and celiac macrophages.

Changes in the amount of pSTAT1 and pSTAT3 during the courses of Py17XL and Py17XNL infections were further analyzed by quantifying the pSTAT levels and calculating the ratio of pSTAT1 or pSTAT3 in the spleen of the infected mice to that in the spleen of the uninfected control mice during the whole course of infection. We observed the inverse dynamic patterns of pSTAT1 and pSTAT3 in the early stage of infection with the two strains of parasites. As shown in Figures 2E and 2F, although both Py17XNL and Py17XL infections induced a maximum activation of STAT1 and STAT3 on the first day of infection, the self-resolving Py17XNL infection induced a pSTAT1-dominant response during the early stage of infection and then switched to pSTAT3-dominance in the later phase with the resolution of parasitemia. In contrast, the lethal Py17XL infection induced a pSTAT3-dominant response during the whole short course with the death of the animals. The pSTAT1/pSTAT3 ratio has been evaluated as an important index for immunoregulation (26, 31, 35, 36), so we analyzed the constituent ratio of pSTAT1 and pSTAT3 in the spleen during the whole course of Py17XNL (Figure 2G) or Py17XL (Figure 2H) infection. The pSTAT1/pSTAT3 ratio was increased during the early stage of Py17XNL infection, peaked on day 7 p.i., and subsequently decreased. But three weeks later, the pSTAT1/pSTAT3 ratio of the infected mice was lower than that of the uninfected control mice (Figure 2G). However, during the whole course of Py17XL infection, the pSTAT1/pSTAT3

ratio of the infected mice was lower than that of the uninfected control mice (Figure 2H). Thus, our results indicated that infections with Py17XNL and Py17XL induced different dynamic patterns of pSTAT1 and pSTAT3 balance.

Immunohistochemistry analysis of activation of STAT1 and STAT3 induced by P. yoelii infection

In order to observe the distribution of pSTAT1/3-positive cells in spleen and in liver, sections, made from spleen and liver collected on the first day post infection with Py17XNL or Py17XL, were stained with HE and immunohistochemically for detecting levels of pSTAT1/3. The numbers of pSTAT1/3-positive cells in spleens (Figure 3) and in livers (Figure 4) of infected mice were more than that of the uninfected control mice. These results were consistent with those of Western blot analysis. The pSTAT1/3-positive cells in spleen dispersed in every region, including white and red pulp, in the two infected groups. The results of pSTAT1/3 staining in spleens in the following days of infection were similar to those of the Western blot analysis (data not shown).

Discussion

We analyzed the kinetics of STAT1 and STAT3 activation in mice during the course of infection with two closely related strains of *P. yoelii*. We observed that both Py17XNL and Py17XL infections induced a maximum activation of STAT1 and STAT3 during early infection. The timing of STAT1 and STAT3 activation observed in this study is unexplainable under the current theory on signal transduction pathways. It is generally believed that pSTAT1 and pSTAT3 are downstream molecules in cytokine signaling pathways (pSTAT1 for IFNs and pSTAT3 for IL-10) (31). In a similar mouse malaria study, IFN-γ and TNF-α reached peak levels between days 5 and 7 in mice following infection with lethal or nonlethal *P. yoelii*. Peak levels of IL-10 appeared on day 16 in nonlethal strain infection and at least by day 7 in lethal malaria (all animals died on day 7 p.i.). Peak levels of TGF-β appeared on day 16 in nonlethal malaria and on day 2 in lethal malaria (12). Our results indicated that maximum activation of STAT1 and STAT3 occurred much earlier than the peak levels of cytokines during malaria infection reported by others (12, 13, 37). It is possible that some malarial parasite molecules, yet to be identified, may directly activate STAT1 and STAT3. STAT1 and STAT3 activation may be the early event during malaria infection; pSTAT1 and pSTAT3 may play an important role in inducing cytokine response. This merits further study.

The present work demonstrated that the clear dynamic changes of pSTAT1 and pSTAT3 occurred in spleen, but not in the mesenteric lymph nodes or celiac macrophages and a dynamic change of pSTAT3 could be observed in liver. These results were consistent with those in previous reports in which the spleen plays a central role in controlling and clearing the parasite (38-40), the liver has some function in the control of malaria (41), but the mesenteric lymph nodes (42) and celiac macrophages (43) are not the main immune organs or cells in immunity against blood stage malaria.

It has been documented that infections with a nonlethal (Py17XNL) and lethal (Py17XL) strain of *Plasmodium yoelii* lead to different outcomes of the disease (12). Our present studies indicated for the first time that these lethal and nonlethal *Plasmodium* strains induced different dynamic patterns of pSTAT1 and pSTAT3 balance in the spleens of the infected mice. The nonlethal strain Py17XNL induced a pSTAT1-dominant response during the early stage of infection, which might cause the final resolution of the infection. But the lethal strain Py17XL induced a pSTAT3-dominant response, which might cause the overwhelming parasitemia and the death of the animals. In the later stage of Py17XNL infection, the pSTAT1-dominance was switched to the pSTAT3-dominance. The "switch" might represent an important mechanism to prevent immunopathology associated with anti-malarial immunity. The STAT3-dominant response during the early phase of Py17XL infection may inhibit the development of protective immunity, leading to high parasitemia and death.

It is known that pSTAT1 is critical in inducing Th1/pro-inflammatory cytokines, activating DC and NK cells, up-regulating MHC class I/II molecules and co-stimulation molecules on immune cells, prolonging the survival of T cells, enhancing the activity of cytotoxic T lymphocytes (CTL), and inhibiting the regulatory T (Treg) cell and anti-inflammatory cytokine (TGF-β and IL-10) responses (26). pSTAT3, which has antagonistic effect on pSTAT1 (27, 28), plays a key role in suppressing the function of neutrophils, NK cells, DCs (31-33) and negatively regulating the Th1-mediated inflammatory response (30, 31). Therefore, the balance of pSTAT1 and pSTAT3 plays an important role in regulating immune response and maintaining immuno-homeostasis. The results presented in this study suggest that the balance of pSTAT1 and pSTAT3 responses may also have an important implication in malaria immunology, meriting further study.

Acknowledgements

We thank Professor Yaming Cao for providing the Py17XNL strain and the Malaria Research and Reference Reagent Resource Center (MR4, MAL88851-01265293) for donating the Py17XL strain of *Plasmodium yoelii*. We also appreciate Quansheng Guan and Liang Zhang for their technical assistance in immunohistochemistry analysis.

References

1. Stevenson MM, Riley EM. Innate immunity to malaria. Nat Rev Immunol. 2004;4:169-180.
2. Stevenson MM, Tam MF, Wolf SF, Sher A. IL-12-induced protection against blood-stage *Plasmodium chabaudi* AS requires IFN-γ and TNF-α and occurs *via* a nitric oxide-dependent mechanism. J Immunol. 1995;155:2545-2556.
3. Stevenson MM, Urban BC. Antigen presentation and dendritic cell biology in malaria. Parasite Immunol. 2006;28:5-14.

4. Su Z, Stevenson MM. Central role of endogenous γ interferon in protective immunity against blood-stage *Plasmodium chabaudi* AS infection. Infect Immun. 2000;68:4399-4406.
5. Tsutsui N, Kamiyama T. Transforming growth factor β-induced failure of resistance to infection with blood-stage *Plasmodium chabaudi* in mice. Infect Immun. 1999;67:2306-2311.
6. Torre D, Speranza F, Martegani R. Role of proinflammatory and anti-inflammatory cytokines in the immune response to *Plasmodium falciparum* malaria. Lancet Infect Dis. 2002;2:719-720.
7. Omer FM, Kurtzhals JA, Riley EM. Maintaining the immunological balance in parasitic infections: a role for TGF-β? Parasitol Today (Personal ed). 2000;16:18-23.
8. Artavanis-Tsakonas K, Tongren JE, Riley EM. The war between the malaria parasite and the immune system: immunity, immunoregulation and immunopathology. Clin Exp Immunol. 2003;133:145-152.
9. Dodoo D, Omer FM, Todd J, Akanmori BD, Koram KA, Riley EM. Absolute levels and ratios of proinflammatory and anti-inflammatory cytokine production *in vitro* predict clinical immunity to *Plasmodium falciparum* malaria. J Infect Dis. 2002; 185:971-979.
10. Li C, Corraliza I, Langhorne J. A defect in interleukin-10 leads to enhanced malarial disease in *Plasmodium chabaudi* chabaudi infection in mice. Infect Immun. 1999;67:4435-4442.
11. Omer FM, Riley EM. Transforming growth factor β production is inversely correlated with severity of murine malaria infection. J Exp Med. 1998;188:39-48.
12. Omer FM, de Souza JB, Riley EM. Differential induction of TGF-β regulates proinflammatory cytokine production and determines the outcome of lethal and nonlethal *Plasmodium yoelii* infections. J Immunol. 2003;171:5430-5436.
13. De Souza JB, Williamson KH, Otani T, Playfair JH. Early γ interferon responses in lethal and nonlethal murine blood-stage malaria. Infect Immun. 1997;65:1593-1598.
14. Torre D, Speranza F, Giola M, Matteelli A, Tambini R, Biondi G. Role of Th1 and Th2 cytokines in immune response to uncomplicated *Plasmodium falciparum* malaria. Clin Diagn Lab Immunol. 2002;9:348-351.
15. Kobayashi F, Ishida H, Matsui T, Tsuji M. Effects of *in vivo* administration of anti-IL-10 or anti-IFN-γ monoclonal antibody on the host defense mechanism against *Plasmodium yoelii* yoelii infection. Melatonin regulates nitric oxide synthase expression in ischemic brain injury. J Vet Med Sci. 2000;62:583-587.
16. Chen WG, Daines MO, Hershey GKK. Turning off signal transducer and activator of transcription (STAT): The negative regulation of STAT signaling. J Allergy Clin Immunol. 2004; 114:476-489.
17. Ihle JN. STATs: signal transducers and activators of transcription. Cell. 1996;84:331-334.
18. Durbin JE, Hackenmiller R, Simon MC, Levy DE. Targeted disruption of the mouse Stat1 gene results in compromised innate immunity to viral disease. Cell. 1996;84:443-450.
19. Meraz MA, White JM, Sheehan KC, et al. Targeted disruption of the Stat1 gene in mice reveals unexpected physiologic specificity in the JAK-STAT signaling pathway. Cell. 1996;84: 431-442.
20. Rosas LE, Keiser T, Pyles R, Durbin J, Satoskar AR. Development of protective immunity against cutaneous leishmaniasis is dependent on STAT1-mediated IFN signaling pathway. Eur J Immunol. 2003;33:1799-1805.
21. Szabo SJ, Sullivan BM, Peng SL, Glimcher LH. Molecular mechanisms regulating Th1 immune responses. Annu Rev Immunol. 2003;21:713-758.
22. Vakkila J, Demarco RA, Lotze MT. Coordinate NF-κB and STAT1 activation promotes development of myeloid type 1 dendritic cells. Scand J Immunol. 2008;67:260-269.
23. Jackson SH, Yu CR, Mahdi RM, Ebong S, Egwuagu CE. Dendritic cell maturation requires STAT1 and is under feedback regulation by suppressors of cytokine signaling. J Immunol. 2004;172:2307-2315.
24. Carson WE, Dierksheide JE, Jabbour S, et al. Coadministration of interleukin-18 and interleukin-12 induces a fatal inflammatory response in mice: critical role of natural killer cell interferon-γ production and STAT-mediated signal transduction. Blood. 2000;96:1465-1473.
25. Wei J, Duramad O, Perng OA, Reiner SL, Liu YJ, Qin FX. Antagonistic nature of T helper 1/2 developmental programs in opposing peripheral induction of $Foxp3^+$ regulatory T cells. Proc Natl Acad Sci U S A. 2007;104:18169-18174.
26. Dunn GP, Koebel CM, Schreiber RD. Interferons, immunity and cancer immunoediting. Nat Rev. 2006;6:836-848.
27. Hong F, Jaruga B, Kim WH, et al. Opposing roles of STAT1 and STAT3 in T cell-mediated hepatitis: regulation by SOCS. J Clin Invest. 2002;110:1503-1513.
28. Gabriella R, Sara P, Daniela B, Francesco N, Valeria P. Ups and downs: the STAT1:STAT3 seesaw of interferon and gp130 receptor signalling. Semin Cell Dev Biol. 2008; in press.
29. Yu H, Jove R. The STATs of cancer--new molecular targets come of age. Nat Rev Cancer. 2004;4:97-105.
30. El Kasmi KC, Holst J, Coffre M, et al. General nature of the STAT3-activated anti-inflammatory response. J Immunol. 2006; 177:7880-7888.
31. Yu H, Kortylewski M, Pardoll D. Crosstalk between cancer and immune cells: role of STAT3 in the tumour microenvironment. Nat Rev Immunol. 2007;7:41-51.
32. Kortylewski M, Kujawski M, Wang T, et al. Inhibiting Stat3 signaling in the hematopoietic system elicits multicomponent antitumor immunity. Nat Med. 2005;11:1314-1321.
33. Takeda K, Clausen BE, Kaisho T, et al. Enhanced Th1 activity and development of chronic enterocolitis in mice devoid of Stat3 in macrophages and neutrophils. Immunity. 1999;10:39-49.
34. Adamkova L, Souckova K, Kovarik J. Transcription protein STAT1: biology and relation to cancer. Folia Biol. 2007;53:1-6.
35. Wang W, Edington HD, Rao UN, et al. STAT3 as a biomarker of progression in atypical nevi of patients with melanoma: dose-response effects of systemic IFNα therapy. J Invest Dermatol. 2008;128:1997-2002.
36. Wang W, Edington HD, Rao UN, et al. Modulation of signal transducers and activators of transcription 1 and 3 signaling in melanoma by high-dose IFNα2b. Clin Cancer Res. 2007;13: 1523-1531.
37. Couper KN, Blount DG, Wilson MS, et al. IL-10 from CD4 CD25Foxp3CD127 adaptive regulatory T cells modulates parasite clearance and pathology during malaria infection. PLoS Pathog. 2008;4:e1000004.
38. Chotivanich K, Udomsangpetch R, McGready R, et al. Central role of the spleen in malaria parasite clearance. J Infect Dis. 2002;185:1538-1541.
39. Oster CN, Koontz LC, Wyler DJ. Malaria in asplenic mice: effects of splenectomy, congenital asplenia, and splenic reconstitution on the course of infection. Am J Trop Med Hyg. 1980;29:1138-1142.
40. Engwerda CR, Beattie L, Amante FH. The importance of the spleen in malaria. Trends Parasitol. 2005;21:75-80.
41. Dockrell HM, de Souza JB, Playfair JH. The role of the liver in immunity to blood-stage murine malaria. Immunology. 1980;41:

421-430.
42. Playfair JH, de Souza JB. Lymphocyte traffic and lymphocyte destruction in murine malaria. Immunology. 1982;46:125-133.
43. Shear HL, Nussenzweig RS, Bianco C. Immune phagocytosis in murine malaria. J Exp Med. 1979;149:1288-1298.